Shear and loading in channels: Oscillatory shearing and edge currents of superconducting vortices

J. F. Wambaugh,[1,2] F. Marchesoni,[3,4] and Franco Nori[1,4,]*

[1]*Center for Theoretical Physics, Department of Physics, and Center for the Study of Complex Systems, The University of Michigan, Ann Arbor, Michigan 48109-1120*
[2]*Department of Physics, Duke University, Durham, North Carolina 27708*
[3]*Istituto Nazionale di Fisica della Materia, Universitá di Camerino, Camerino, I-62032, Italy*
[4]*Frontier Research System, The Institute of Physical and Chemical Research (RIKEN), Saitama 351-0198, Japan*

Via computer simulations we study the motion of quantized magnetic flux-lines, or vortices, confined to a straight pin-free channel in a strong-pinning superconducting sample. We find that, when a constant current is applied across this system, a very unusual oscillatory shearing appears, in which the vortices moving at the edges of the channel periodically trail behind and then suddenly leapfrog past the vortices moving in the inner rows. For small enough driving forces, this oscillatory shearing dynamic phase is replaced by a continuous shearing phase in which the distance between initially-nearby vortices grows in time, quickly destroying the order of the lattice. An animation of this novel ''oscillatory leapfrogging shear'' effect of the vortex edge currents appears in http://www-personal.engin.umich.edu/~nori/channel/

I. INTRODUCTION

Flux pinning in type II superconductors is of both technological and scientific interest. While most experiments focus on the effects of random pinning distributions, a growing number of investigations have been carried out on artificially structured samples, including periodic arrays of pinning sites and channels. In this paper we will study vortex motion inside channels.

A. Recent work on vortex motion in channels

van der Drift *et al.* have done very systematic studies of the motion of vortices in channels, including the fabrication of the channel samples and preliminary results;[1] studies of vortex shear and matching effects in straight[2] and curved channels;[3] channels in BSCCO (Ref. 4), vortex viscosity in the liquid state and finite size melting,[5] and matching effects on straight channels.[6] These studies revealed a plethora of novel and interesting vortex dynamic effects. For example, Ref. 6 recently found incommensurate easy flow channels in an otherwise perfect flux lattice. This study, which also included a comparison with the Frenkel-Kontorova model,[7] found that the associated point defects in the lattice inside the channel cause an almost vanishing critical current. In addition to the normal flux flow behavior, they found a low mobility regime at small drives associated with defect motion. The authors of Ref. 8 also obtained striking direct observations of such vortex flow ''channels'' using magnetic decoration experiments on NbSe2 single crystals.

Anders and co-workers[9–11] have done remarkable studies of vortex transport, including vortex noise, in thin film samples containing very narrow channels of various geometries. The samples are somewhat similar to the ones studied in Ref. 5. In their recent experiments with ultrathin layers[11] vortex matter was sheared along nanofabricated flow channels. The vortex ''lattice'' structure inside the channels can be tuned continuously by changing the applied magnetic field. The configurations obtained vary from perfectly ordered, to totally amorphous. They also analyzed the changes in the static and dynamic response in terms of an effective static and dynamic friction.

Kwok *et al.*[12] irradiated samples creating strong-pinning stripes where the motion of vortices can be channeled and studied via systematic transport measurements. Interesting theoretical work on vortex matter in confined geometries can be found in Refs. 13 and 14.

Using a modified version of the simulations in Refs. 15 and 16, we have recently proposed[17] interesting types of vortex channels that can be used for vortex optics, including vortex lenses and flux pumps. More specifically, we proposed the concept of two-dimensions asymmetric channel walls to provide an experimentally-realizable way to easily move vortices through channels in ac-driven devices.[17] These asymmetric channels would allow, for example, the construction of concave/convex vortex lenses that concentrate/disperse vortices in nanodevices and also remove unwanted trapped flux in superconducting quantum interference devices.[18]

The recent and ongoing studies listed above have uncovered novel aspects of vortex motion in restricted geometries. Here we will focus on molecular dynamics simulations of vortices inside straight channels, characterization of several new dynamic phases. Other related topics (e.g., curved channels, recovery of the hydrodynamic limit for growing number of vortices, etc.) are outside the scope of this paper.

B. Overview of this work

The typical configuration considered here consists of vortices driven along a zero-pinning channel, surrounded by fixed vortices, due to the very strong pinning present outside the channel. The longitudinal motion of vortices along the
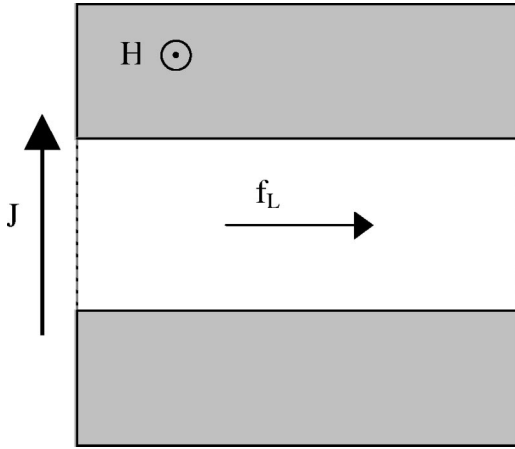
FIG. 1. Schematic diagram of the top view of the simulated sample. Gray regions have very strong pinning, while the white channel has zero pinning.

channel is due to a longitudinal Lorentz force transverse is schematically shown in Fig. 1.

If a weak-pinning or pin-free channel is continuously *loaded*, or driven, with vortices, they will shear[19] with the pinned rows of vortices located right outside the channel. This work studies the dynamics of vortices moving in channels. Our main finding is that vortex motion in the channel can exhibit several unusual dynamic phases, including *oscillatory shearing* of the edge rows of vortices. In this latter phase, the outer moving rows, or *edge currents* of vortices, first trail behind the central vortex lanes of this "fluxon-bahn," then leapfrog ahead of the other moving vortices, remaining there for a short period of time before slowing down to the same velocity as the central rows, and finally trailing behind—starting the "oscillatory shearing" cycle of the edge currents all over again. Thus, in this oscillatory shearing dynamic phase, the distance between initially nearby vortices periodically oscillates in time, and does not grow indefinitely. This phase is ubiquitous and has been observed for numerous vortex densities and driving forces. At low drives, however, the flux lattice does not exhibit oscillatory shearing, but only *continuous shearing* and the distance between initially nearby vortices grows in time, thus destroying the order of the vortex lattice.

It is important to emphasize that the pinned vortices just outside the channel create an "egg carton" or "periodic bottleneck" potential at the channel edges. It is this potential that is responsible for the "stick-slip" motion (or, more precisely "lag-leapfrog," or "slow-down-and accelerate" periodic cycles) of the moving vortices described in this paper. Indeed, *all the vortex velocity oscillations* shown in this paper *originate from the oscillatory drag produced by this periodic bottleneck.*

II. SIMULATION

Computer simulations were performed using a new version of the molecular dynamics (MD) code previously used for systems with random[15] and correlated[16] pinning. Other types of MD studies have been done by other groups (see, for

instance, Ref. 20). We model a transverse two-dimensional (2D) slice (in the x-y plane) of an infinite zero-field-cooled superconducting slab containing current-driven 3D rigid vortices that are parallel to the sample edge. The samples have very strong, effectively infinite, pinning everywhere except the zero-pinning central channel (see Fig. 1). In the latter, vortices move subject to fluxon-vortex repulsions $\mathbf{f}_{vv}$, an externally applied ac Lorentz driving force $\mathbf{f}_L$, and interactions with the channel boundaries. Thus, inside the channel, the total force on a vortex is

$$\mathbf{f} = \mathbf{f}_{vv} + \mathbf{f}_L = \eta \mathbf{v}, \tag{1}$$

where the total force on vortex i due to other vortices is given by

$$\mathbf{f}_{vv}^{(i)} = \sum_{j=1}^{N_v} f_0 K_1\left(\frac{|\mathbf{r}_i - \mathbf{r}_j|}{\lambda}\right) \hat{\mathbf{r}}_{ij}. \tag{2}$$

Here, K_1 is a modified Bessel function, $\mathbf{r}_i$ ($\mathbf{v}_i$) is the location (velocity) of the ith fluxon, N_v is the number of vortices, $\hat{\mathbf{r}}_{ij} = (\mathbf{r}_i - \mathbf{r}_j)/|\mathbf{r}_i - \mathbf{r}_j|$, and we take $\Delta t = 0.01$, $\tau \equiv 1/\Delta t$ MD steps, and $\eta = 1$. Unless otherwise noted, $\tau = 100$ MD steps. Results do not depend on the choice of Δt, as long as this is small enough. For instance, for the animation in our web site, we have used $\Delta t = 0.001$. We measure all forces in units of

$$f_0 = \frac{\Phi_0^2}{8\pi^2\lambda^3}, \tag{3}$$

magnetic fields in units of Φ_0/λ^2, and lengths in units of the penetration depth λ. Here, $\Phi_0 = hc/2e$ is the flux quantum.

Unless otherwise specified, each figure refers to simulations conducted in the following way: Initially vortices were placed uniformly across the sample in a minimum-energy, field-cooled triangular lattice and the vortices in the channel were subjected to a current along y; producing a Lorentz driving force,

$$F \equiv \frac{f_L}{f_0}, $$

along x.

The square sample had side 18λ and the central straight channel was parallel to the x-axis, centered in the sample and 7λ wide. The zero-pinning central channel starts from the $y = 6$ (λ wide) bin to the $y = 12$ bin, both included. This configuration is schematically depicted in Fig. 1. The initial triangular distribution resulted in roughly two thirds of the vortices being fixed in the very strong pinning region outside the central channel. The square sample had periodic boundary conditions, allowing free vortices in the channel to continue moving along the x axis indefinitely. Because of the channel walls, periodic boundary conditions along the y axis did not affect the dynamics.

III. VORTEX VELOCITIES INSIDE THE CHANNEL

Initially, 80 vortices were placed in a triangular lattice on the sample with a straight central channel. This resulted in roughly one third of the vortices being in a free channel lined
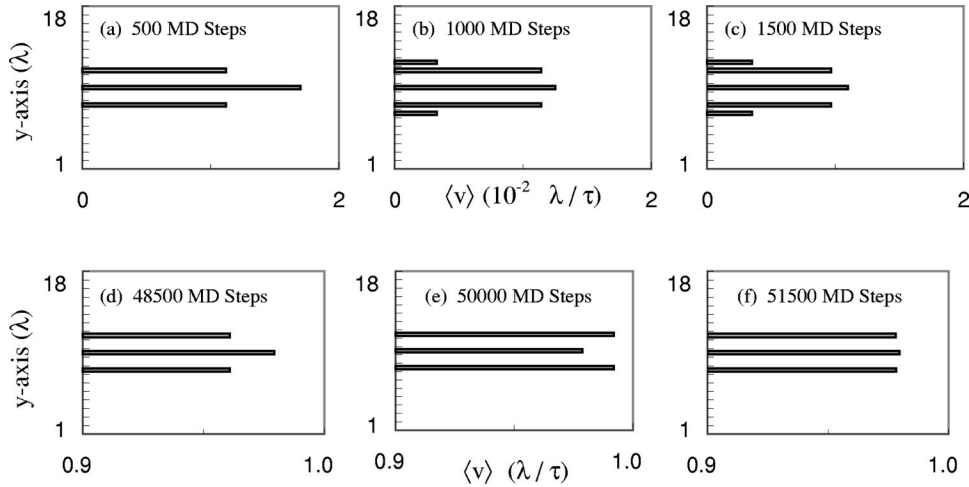
FIG. 2. Velocity of vortices moving inside the sample for several (one λ-wide) bins along the *y*-axis of the sample. Two separate sequences, (a)–(c) and (d)–(f), are shown, corresponding to $F=0.02$ and $F=1$, respectively. These frames show successive snapshots of the velocity of the vortices (integrated along *x*, and binned along *y*). In (a)–(c) the ''edge currents'' of vortices trail behind the central vortex lanes of this ''fluxon-bahn.'' This data clearly shows, in (d)–(f), that the average velocity of the edge current of vortices first trails behind the central vortices (d), then leapfrogs ahead (e), remains there for a short period of time, and then slows down reaching the same velocity of the central rows (f), until finally trails behind—starting the cycle all over again. Notice that the time between the successive snapshots in (a)–(c) is 500 MD steps, while the time between successive snapshots in (d)–(f) is 1,500 MD steps. The number of MD steps between ''binned velocity snapshots'' reflects our chosen sampling rate, and not anything inherent to the period of velocity oscillations.

with pinned vortices, with the free vortices distributed in three rows of eight vortices each. Higher densities of vortices were also considered, and one of these higher-field results will be presented in the next section.

When an applied continuous current drove the free vortices in the *x*-direction, the free vortices near the edges of the channel interacted with the egg carton potential produced by the fixed vortices in the pinned region outside the channel. Intuition would expect this situation to produce drag, resulting in a slightly higher velocity for vortices near the middle of the channel. Examinations of the velocity profiles, depicted in Figs. 2(a)–2(c), show that this is indeed the case, but only for small enough driving forces. For large drives, a nonintuitive oscillating sheared phase Figs. 2(d)–2(f) takes place. Figure 2 shows a ''velocity profile'' computed by

$$\langle v \rangle (y) = \frac{1}{N(y)} \sum_{i_y=1}^{N(y)} v_{i_y}(y), \qquad (4)$$

which is a discrete version of

$$\langle v \rangle (y) = \frac{1}{L_x} \int_0^{L_x} dx\, v(x,y) \qquad (5)$$

In the equations above, $N(y)$ is the number of vortices in the bin between *y* and $y+\Delta y$, where we have chosen $\Delta y = \lambda$; i_y labels the bins along the *y* axis. The horizontal length of the channel is $L_x = 18\lambda$.

We want to monitor the time evolution of $v(y)$, since shear implies a non-zero gradient along *y* of $v(y)$. We have found that binned velocity snapshots, like the ones shown in Fig. 2, are useful because they illustrate the shear-induced presence of gradients in $v(y)$. Thus, we binned the vortex velocity along *y* and integrated the velocities along *x*.

The two sequences [(a)–(c) and (d)–(f) in Fig. 2] of velocity profiles across a channel are successive velocity snapshots. These snapshots are made every 500 MD steps during the course of a simulation: (a)–(c) shows three successive snapshots, while in (e)–(f) every third snapshot is shown. These two particular chronological sequences show two different types of behaviors that we have found when a perfect triangular lattice of vortices is placed and then forced to move on a superconducting sample with a straight channel.

A. Continuously sheared dynamic phase for low driving

Sequence (a)–(c) in Fig. 2 corresponds to a relatively weak driving force of magnitude $F=0.02$, and displays the expected ''beer-belly'' curved velocity profile. Here the shear between the edge vortices of the channel and the pinned vortices outside the channel induces a curvature in the velocity profile. The zero-pinning central channel starts from the $y=6$ (λ-wide) bin to the $y=12$ bin, both included. These bins are occasionally occupied, depending on the pressure exerted on the edge channels of vortices. In (a), the edge rows, interacting with the infinitely pinned vortices experience drag, resulting in the inner row moving slightly faster. The interaction between the inner (bin 9) and outer (bins 7 and 11) vortex rows pulls the outer rows along, eventually pushing outwards a few vortices in the edge rows—as they catch on the pinned vortex potential, as shown in Fig. 2(b). This outward displacement of a few edge vortices creates defects in the moving vortex lattice and also the appearance, in the velocity profile in Fig. 2(b), of moving vortices (in bins 6 and 12) where there were previously none. For this low density of vortices, and for our chosen fine-grained bins, there are no vortices in bins 8 and 10. A higher density example will be discussed below. In Fig. 2(c), the velocity
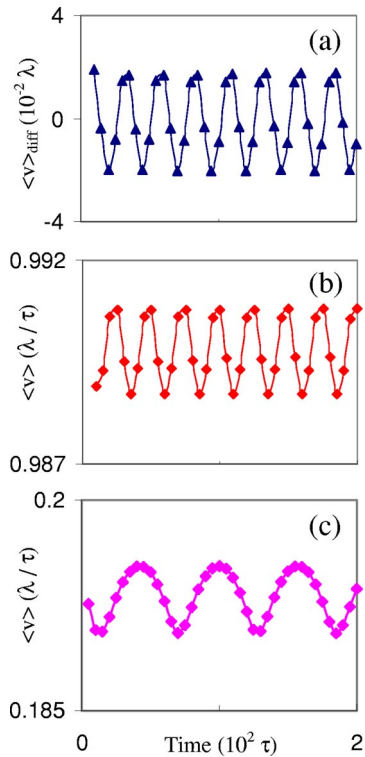
FIG. 3. Comparison of the average velocities of the entire moving vortex lattice (a), and the difference between the velocities of the inner and outer rows of vortices (b). (a) and (b) refer to the same run with 80 vortices. However, (c) uses 340 vortices, instead of the 80 used to obtain (b). Notice that (a) and (b) are correlated with the same frequency, but phase shifted by about $3\pi/4$.

profile has remained "fanned out" as the vortices continue to be driven. The original triangular lattice arrangement has not been preserved because the vortex lattice has been continuously sheared, producing many defects. Indeed, the distance between initially nearby vortices grows with time, for low driving forces.

B. Oscillatory shearing dynamic phase for higher driving

At a higher driving force, however, a novel dynamic vortex phase is observed. Sequence (d)–(f) in Fig. 2 has the same number of vortices as in (a)–(c), but driven by a higher driving force; $F=1$ instead of $F=0.02$. Now, instead of allowing vortices to slip from the outer rows as they catch on the interactions with pinned vortices, the outer rows of vortices actually leapfrog forward past the inner row, by temporarily moving more rapidly than the inner row. Here, (e) clearly shows the outer rows actually move faster than the inner rows. Eventually, the faster edge rows slow down and, as shown in (f), this results in a brief effective uniform velocity across the channel.

This unexpected cycle repeats periodically and it is even more pronounced when there are higher vortex densities, corresponding to higher magnetic fields. The three-row arrangement shown here is just the simplest example that illustrates this novel vortex dynamic phase.

To further characterize this dynamics, Fig. 3 shows the temporal evolution of the difference in velocities v_{diff} between the inner and outer rows (a). The overall average velocity in the channel has also been plotted, in (b) to show how v_{diff} correlates to v. The latter will be discussed more in Sec. V. The velocity in (b) changes to (c) when the number of vortices is increased from 80 to 340.

IV. LEAPFROGGING EDGE VORTICES AT HIGHER VORTEX DENSITIES

The very unusual cycle of "trail-behind" and leapfrogging edge vortices seen in Fig. 2 very clearly persists at much higher field strengths, as indicated in Fig. 4. There, the density of vortices is about four times higher than in the case shown in Fig. 2. When we say "leapfrog" we are referring to velocity space, and not necessarily the actual movement of the outer rows past the inner rows.

The chronological sequence of "snapshots" in velocity space in Fig. 4 depicts the time evolution of the velocity of vortices across the channel. This situation is similar to Figs. 2(d)–2(f), but now there is a much higher field strength: 340 vortices have now been placed in a triangular lattice on the sample with a straight central channel. This combination of field strength and channel width results in the channel being filled with seven horizontal rows of seventeen vortices each.

The behavior exhibited in Fig. 4 is the result of inner rows of vortices being locked together with the outer rows, despite the interactions of the outer rows with the pinned vortices outside the zero-pinning channel. Intuitively one would expect that profiles like (a), (b) and (f) are the norm: *The outer rows snag on the pinned vortices and lag behind the less restricted inner rows*. The surprising behavior is that profiles like (c) and (d) indicate that *the temporarily jammed or slowed-down vortices in the outer rows suddenly "catch up" or leapfrog by momentarily exceeding the velocity of vortices in the inner rows*. Panel (e) in Fig. 4 shows that this can also result in a much flatter velocity profile than otherwise expected, albeit just briefly.

Simulations at both field strengths discussed here (80 and 340 vortices on the sample) demonstrate continuous shearing under low driving forces, but unusual oscillatory shearing under higher driving forces. In addition to higher field strengths, simulations with smaller Δt's were used, producing the same results (e.g., 0.001 instead of 0.01). An animation showing the change in velocity profile during a simulation with small Δt is available on the web.[21]

V. VELOCITY VERSUS TIME FOR SEVERAL DRIVING FORCES

Figure 5 shows the vortex velocity, now averaged over the entire sample, for the oscillating shearing phase (top curve, $F=1$), the continuous shearing phase (bottom curve, $F=0.02$), and an intermediate "ramped driving" case, where the driving force is slowly increased to monitor the crossover (not a sharp dynamic phase transition) between these two dynamic phases. Several simulations were performed, but only three representative ones are shown here.

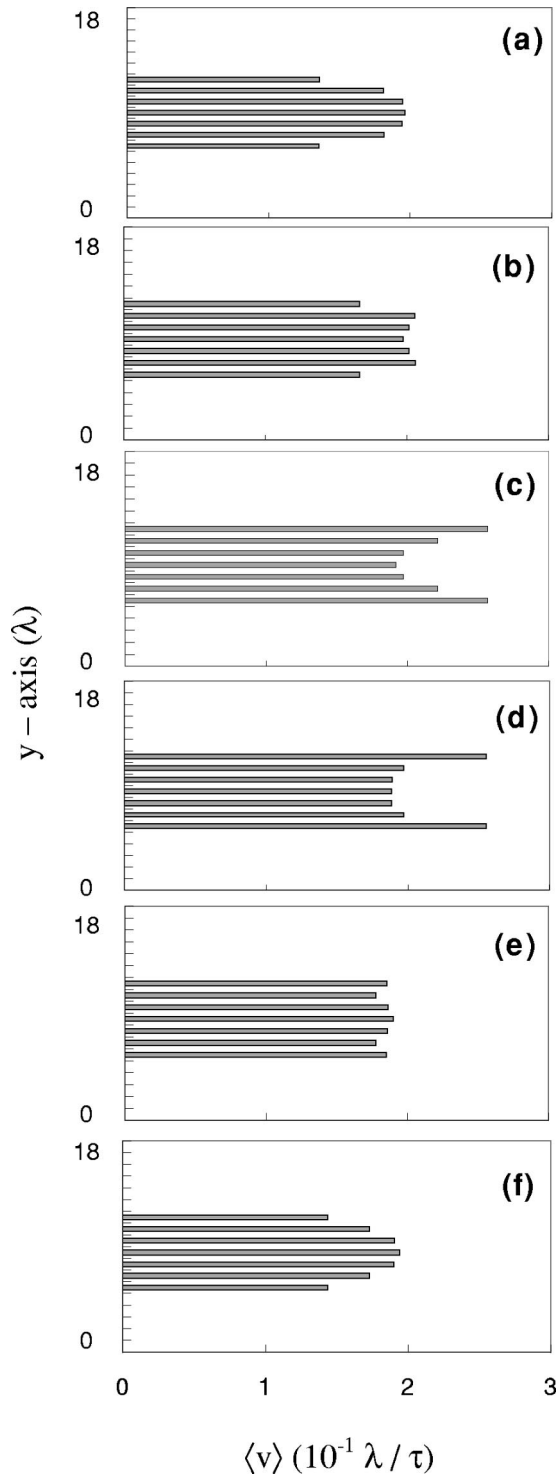Eighty vortices were placed in a triangular lattice, with

FIG. 4. Velocity of vortices moving inside the sample for several (one λ wide) bins along the y-axis of the sample. As in Figs. 2(d)–2(f), $F=1$; however, now there are 340 vortices in the sample, instead of just 80. These frames show successive snapshots of the velocity of the vortices (integrated along x, and binned along y). There are 500 MD steps between successive snapshots. Notice how the unusual oscillating shearing (i.e., the gradient along y in the velocity) varies with time across the rows.

rows of fixed vortices bordering the channel of movable ones. The egg carton type effective interaction of the free vortices in the channel with the nearby pinned ones yields several dynamic phases, including the unusual oscillating shearing dynamic phase illustrated in Fig. 2(e).

The lowest curve shown in Fig. 5 corresponds to a weak-driving case; here with force $F=0.02$. First, there is a transient. Afterwards, the average velocity of the entire lattice, not just the edge vortices anymore, shows marked oscillations with time. This corresponds to a "stick-slip-type" motion of the vortex lattice *impinging upon a succession of potential energy bottlenecks as it is pushed through the channel*. Notice that, strictly speaking, the "stick" phase is really moving, and never stuck. Thus, it is more appropriate to describe it as a phase with an oscillating sine-like average velocity. Notice also that the velocity oscillations in this low-driving "continuous shearing" dynamic phase span about 1/3 of an order of magnitude (the vertical axis has a logarithmic scale).

The highest curve in Fig. 5 shows a typical large-driving, $F=1$, case. There, the system is in the oscillating shearing dynamic phase, and the average velocity of the entire system oscillates, as shown in the magnification of this plot located in the lower right inset. The average velocity appears to be constant in the main panel of Fig. 5 because its vertical axis spans five decades!

To monitor the crossover between these two dynamic phases, Fig. 5 also shows an intermediate curve, where the driving force was *slowly* increased from an initial value of $F=0.02$ to a final value of $F=1$. While the average velocity oscillations of the continuous shearing phase, the low-driving-force-regime, initially persist, it is clear that the amplitude of the velocity oscillations decreases until there is no discernable oscillation (without magnification) in the logarithmic plot. In other words, when the average velocity of the moving vortices is plotted over time, while the driving force is slowly increased, the average velocity eventually becomes relatively stable, in the sense that there is not much overall relative shifting in the lattice. Thus, the lattice, while sheared with oscillating velocities, is not completely torn apart at higher driving forces—because of the periodic "leapfrog" jumps of the trailing edge vortices.

For the measurements shown in Fig. 5, the average displacement of all moving vortices was recorded every 500 MD steps, over the course of 250 000 MD step simulations. We also studied many more values for the driving force, including very high values. For all cases where F was approximately larger than 0.05, oscillating shearing was found.

Since the oscillations in the average velocity are caused by the interaction between the moving and pinned vortices, we have found that the frequency of the oscillations depends on the density of the vortices (they are inversely proportional). Thus, careful measurements of the average velocity (e.g., as a voltage), might provide an indirect way of determining the vortex density and magnetic field strength. Indeed, in Fig. 3, the system that produces the signal (c) is the same one as in (b) but with about four times the number of vortices. Notice how the period decreases. Admittedly, this is not the most direct way to measure fields inside channels.
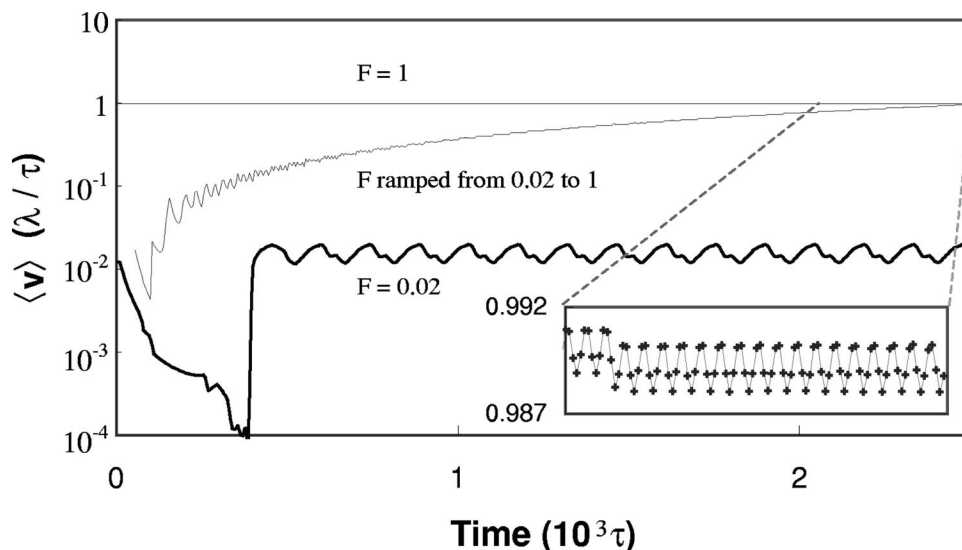
FIG. 5. Time evolution of the vortex velocity, now averaged over the *entire* sample. Every data point corresponds to an average over 500 MD steps. Each run involves 250 000 MD steps. Top curve: for $F=1$, the strong driving case, the total velocity of the vortex lattice oscillates, as shown in the lower right inset. The velocity appears constant because the vertical axis spans five decades. Bottom curve: weak driving case, $F=0.02$, where the system is in the continuous shearing phase. Here the average velocity oscillates after an initial transient. Middle curve: the driving force is linearly ramped up from 0.02 to 1. After an initial transient, the system exhibits a crossover (not a sharp dynamic phase transition) from continuous shearing to oscillatory shearing. The initial points of the transient are not shown because the initial velocity is too low (below 10^{-4}).

VI. CONCLUDING REMARKS

Superconductor vortex channels have been made experimentally using several techniques, including electron beam lithography, irradiation, evaporating layers, or by etching a channel in a strong pinning material (the thinner channel would have less pinning). These recent and ongoing experiments are revealing new physics produced by the vortex dynamics in confined geometries.

More elaborate channels have recently been proposed[17] for transporting vortices along complex nanofabricated channels. These weak-pinning channels with assymetric walls could be very important to get rid of unwanted, trapped flux in superconducting quantum interference device (SQUID) magnetometers, and also move vortices along channels in devices.[18] These promising concepts are largely unexplored, and constitute an open and potentially useful area.

In this work we have studied dynamic phases of vortices confined inside pin-free channels surrounded by a strong pinning material. Our main finding is that vortex motion in the channel can exhibit several novel dynamic phases. The most unusual one involves the leapfrogging of edge vortices producing "oscillatory shearing" of the edge rows of vortices. In this dynamic phase, the distance between initially nearby vortices periodically oscillates in time. At low driving forces, however, the flux lattice exhibits "continuous shearing" and the distance between initially nearby vortices grows in time, thus destroying the order of the vortex lattice. These phases might be best observed using direct imaging methods, like Lorentz microscopy.[22,23]

*Corresponding author. Email address: nori@umich.edu

[1] E. van der Drift, S. Radelaar, A. Pruymboom, and P. H. Kes, J. Vac. Sci. Technol. B **6**, 297 (1988).

[2] A. Pruyjmboom, P. H. Kes, E. van der Drift, and S. Radelaar, Phys. Rev. Lett. **60**, 1430 (1988).

[3] A. Pruymboom, P. H. Kes, E. van der Drift, and S. Radelaar, Appl. Phys. Lett. **52**, 662 (1988).

[4] H. Pastoriza and P. H. Kes, Phys. Rev. Lett. **75**, 3525 (1995).

[5] M. H. Theunissen, E. Van der Drift, and P. H. Kes, Phys. Rev. Lett. **77**, 159 (1996).

[6] R. Besseling, R. Niggebrugge, and P. H. Kes, Phys. Rev. Lett. **82**, 3144 (1999).

[7] L. M. Floria and J. J. Mazo, Adv. Phys. **45**, 505 (1996).

[8] M. Marchevsky, J. Aarts, P. H. Kes, and M. V. Indenbom, Phys. Rev. Lett. **78**, 531 (1997).

[9] S. Anders, Ph.D. thesis, University of Chicago, 1999.

[10] S. Anders, A. W. Smith, H. M. Jaeger, R. Besseling, P. H. Kes, and E. van der Drift, Physica C **332**, 35 (2000).

[11] S. Anders, A. W. Smith, H. M. Jaeger, R. Besseling, P. H. Kes, and E. van der Drift, Phys. Rev. B **62**, 15 195 (2000).

[12] W. Kwok *et al.* (unpublished).

[13] A. Koshelev, Physica C **223**, 276 (1994).

[14] M. C. Marchetti and D. R. Nelson, Physica C **330**, 105 (2000).

[15] F. Nori, Science **278**, 1373 (1996); T. Matsuda, K. Harada, H.

Kasai, O. Kamimura, and A. Tonomura, *ibid.* **278**, 1393 (1996); K. Harada, O. Kamimura, H. Kasai, T. Matsuda, A. Tonomura, and V. V. Moshchalkov, *ibid.* **274**, 1167 (1996); A. Brass, Y. Brechet, and A. J. Berlinsky, Phys. Rev. B **38**, 9235 (1988); R. Richardson, O. Pla, and F. Nori, Phys. Rev. Lett. **72**, 1268 (1994); C. Reichhardt, C. J. Olson, J. Groth, S. Field, and F. Nori, Phys. Rev. B **53**, R8898 (1996); *ibid.* **52**, 10 441 (1995); C. J. Olson, C. Reichhardt, J. Groth, S. B. Field, and F. Nori, Physica C **290**, 89 (1997); C. J. Olson, C. Reichhardt, and F. Nori, Phys. Rev. B **56**, 6175 (1997); Phys. Rev. Lett. **80**, 2197 (1998); **81**, 3757 (1998); C. J. Olson, C. Reichhardt, B. Jankó, and F. Nori, *ibid.* **87**, 177002 (2001); J. Groth, C. Reichhardt, C. J. Olson, S. Field, and F. Nori, *ibid.* **77**, 3625 (1996).

[16] C. Reichhardt, C. J. Olson, and F. Nori, Phys. Rev. B **58**, 6534 (1998); **57**, 7937 (1998); Phys. Rev. Lett. **78**, 2648 (1997); C. Reichhardt and F. Nori, *ibid.* **82**, 414 (1999); C. Reichardt, C. J. Olson, J. Groth, S. Field, and F. Nori, Phys. Rev. B **54**, 16 108 (1996); **56**, 14 196 (1997).

[17] J. F. Wambaugh, C. Reichhardt, C. J. Olson, F. Marchesoni, and F. Nori, Phys. Rev. Lett. **83**, 5106 (1999).

[18] *SQUID Sensors*, edited by H. Weinstock (Kluwer, Dordrecht, 1996); *Superconducting Electronics*, edited by H. Weinstock and M. Nisenoff (Springer, Heidelberg, 1989); H. Weinstock, Physica C **209**, 269 (1993); IEEE Trans. Magn. **27**, 3231 (1991).

[19] F. Nori (unpublished); D. Arovas, Ph.D. thesis, University of California, Santa Barbara, 1986.

[20] E. H. Brandt, J. Low Temp. Phys. **28**, 263 (1977); **28**, 291 (1977); H. J. Jensen, A. Brass, A. C. Shi, and A. J. Berlinsky, Phys. Rev. B **41**, 6394 (1990); H. J. Jensen, Y. Brechet, and A. Brass, J. Low Temp. Phys. **74**, 293 (1989).

[21] Additional information, including videos, appear in http://www-personal.engin.umich.edu/~nori/channel/

[22] A. Tonomura, Physica B **280**, 227 (2000); Int. J. Impact Eng. **15**, 3427 (2000); Mater. Charact. **42**, 201 (1999); Micron **30**, 479 (1999); Phys. Scr. **T76**, 16 (1998); A. Tonomura, H. Kasai, O. Kamimura, T. Matsuda, K. Harada, J. Shimoyama, K. Kishio, and K. Kitazawa, Nature (London) **6717**, 308 (1999); A. Tonomura, H. Kasai, O. Kamimura, T. Matsuda, K. Harada, Y. Nakayama, J. Shimoyama, K. Kishio, T. Hanaguri, K. Kitazawa, M. Sasase, and S. Okayasu, *ibid.* **6847**, 620 (2001); C. H. Sow, K. Harada, A. Tonomura, G. Crabtree, and D. G. Grier, Phys. Rev. Lett. **60**, 2693 (1998); N. Osakabe *et al.*, *ibid.* **78**, 1711 (1997).

[23] After this work was completed, several publications appeared focusing on related systems, including: the paper titled ''Oscillating rows of vortices in superconductors,'' by T. Matsuda, O. Kamimura, H. Kasai, K. Harada, T. Yoshida, T. Akashi, A. Tonomura, Y. Nakayama, J. Shimoyama, K. Kishio, T. Hanaguri, and K. Kitazawa, Science **294**, 2136 (2001); the work ''A one-dimensional chain state of vortex matter'' by A. Grigorenko, S. Bending, T. Tamegai, S. Ooi, and M. Henini, Nature (London) **414**, 728 (2001); and also A. Tonomura, H. Kasai, O. Kamimura, T. Matsuda, K. Harada, Y. Nakayama, J. Shimoyama, K. Kishio, T. Hanaguri, K. Kitazawa, M. Sasase, and S. Okayasu, Nature (London) **412**, 620 (2001). Previous related work by R. Surdeanu, R. J. Wijngaarden, R. Griessen, J. Einfeld, and R. Wördenweber, Europhys. Lett. **54**, 682 (2001), finds that ''Both commensurate and incommensurate channels are observed as well as hopping between channels, in agreement with numerical simulations.'' Some of these channels studied in these works are formed by Josephson vortices, while other vortex channels are formed by a periodic array of pinning sites. These recent papers are evidence of the current interest in the area of ''vortex motion in channels.''